

1 **CRISPR/Cas12a-mediated ultrasensitive and on-site monkeypox**

2 **viral testing**

3 Furong Zhao^{a, 1}, Pei Wang^{a, b, 1}, Haoxuan Wang^{a, 1}, Sirui Liu^a, Muhammad Sohail^a,

4 Xing Zhang^a, Bingzhi Li^{a, *}, He Huang^{a, *}

5 ^a School of Food Science and Pharmaceutical Engineering, Nanjing Normal

6 University

7 ^b School of Life Sciences, Nanjing Normal University, Nanjing 210023, China

8 ¹ Equal contributions:

9 F.Z, P.W, and H.W. contributed equally to this work.

10 * Corresponding Author:

11 Bingzhi Li (bingzhili@njnu.edu.cn)

12 He Huang (huangh@njnu.edu.cn)

13

14 **Abstract**

15 The unexpected transmission of monkeypox virus (MPXV) from Central and
16 West Africa to previously non-endemic locations is triggering a global panic. The
17 ultrasensitive, rapid, and specific detection of MPXV is crucial for controlling its
18 spreading, while such technology has rarely been reported. Herein, we proposed an
19 MPXV assay combining recombinase-aided amplification (RAA) and
20 CRISPR/Cas12a for the first time. This assay targeted MPXV *F3L* gene and yielded a
21 low detection limit (LOD) of 10^1 copies/ μ L. Deriving from the high specificity nature
22 of RAA and CRISPR/Cas12a, through rational optimizations of probes and conditions,
23 this assay showed high selectivity that could distinguish MPXV from other orthopox
24 viruses and current high-profile viruses. To facilitate on-site screening of potential
25 MPXV carriers, a kit integrating lateral flow strips was developed, enabling
26 naked-eye MPXV detection with a LOD of 10^4 copies/ μ L. Our RAA-Cas12a-MPXV
27 assay was able to detect MPXV without the need for sophisticated operation and
28 expensive equipment. We envision that this RAA-Cas12a-MPXV assay can be
29 deployed in emerging viral outbreaks for on-site surveillance of MPXV.

30 **Keywords:** CRISPR; Cas12a; Monkeypox; Nucleic acid testing; Point-of-care testing

31

32 **Introduction**

33 As a member of the genus orthopoxvirus (OPXV) in the family *Poxviridae*,
34 monkeypox virus (MPXV) is a double-stranded DNA (dsDNA) virus firstly isolated
35 in 1958.¹⁻³ Monkeypox was not recognized as a zoonotic disease until the first human
36 case discovered in a 9-month-old boy in Zaire (now the Democratic Republic of the
37 Congo) in 1970.⁴⁻⁶ Animal-to-human transmission of MPXV can occur via humans'
38 close contact with infected animals while human-to-human transmission includes
39 contact with bodily fluids, respiratory droplets, and lesion materials of the infected
40 individual, sexual transmission, and maternal-infant transmission.^{7, 8} Since the first
41 human case, monkeypox has become predominantly endemic in Central and West
42 Africa, for example, Nigeria experienced a large monkeypox outbreak in 2017, with
43 relevant cases continuously emerging.⁹⁻¹¹ It was not until 2003 that the first case
44 occurred in the United States, mainly due to the importation of infected pet prairie
45 dogs from Ghana. Since 2018, monkeypox has also been reported in tourists from
46 Nigeria to other non-endemic countries, involving Israel,¹² the United Kingdom,^{13, 14}
47 Singapore,¹⁵ the United States of America,^{16, 17} and others.¹⁸ Disturbingly, the World
48 Health Organization (WHO) has collected a total of 71,237 laboratory-confirmed
49 cases and 1,097 probable cases from 107 infected member countries since 1 January
50 2022, and declared this outbreak a public health emergency of international concern.¹⁹
51 It has become a new reality that human monkeypox is no longer a rare zoonotic
52 disease, which deserves more public health attention.²⁰ Thus, the detection of
53 monkeypox matters even more in the current post-COVID, more vigilant world.²¹

54 Currently, the MPXV testing relies on methods including polymerase chain
55 reaction (PCR),²²⁻²⁴ enzyme-linked immunosorbent assay (ELISA),^{25, 26}
56 loop-mediated isothermal amplification (LAMP),²⁷ and microarray.^{28, 29} PCR,
57 recognized as the gold standard for the diagnosis of various diseases including
58 monkeypox, displays high accuracy and sensitivity, yet its application in low-resource
59 areas is limited due to its requirements for expensive equipment and skilled
60 operators.³⁰ ELISA may fail in providing MPXV-specific analysis for the
61 serologically cross-reactive characteristic of OPXV and lead to false positive results
62 for recent or remote vaccination.³¹ LAMP is free from precise thermo-cycling, but it
63 suffers from complicated primer design, false positives, and poor quantitative
64 performance. Besides, the microarray method has been developed for the detection
65 and discrimination of OPXV species; however, its practicality and accessibility is
66 limited deriving from high cost and long detection time.³² Therefore, low-cost,
67 ultrasensitive, and rapid methods that can facilitate on-site and facile MPXV detection
68 have remained elusive.

69 CRISPR/Cas (clustered regularly interspaced short palindromic repeats and
70 CRISPR-associated protein) discovered in the adaptive immune system of
71 prokaryotes, was initially proposed as a revolutionary gene editing technology and
72 later expanded to the fields of molecular diagnosis and biosensing.^{33, 34}
73 CRISPR/Cas12a system that integrates biorecognition (Cas12a crRNA binding to the
74 target) with signal transduction (activated Cas12a indiscriminately cleaving any
75 surrounding single-stranded DNA reporters) has participated in the detection of

76 various viruses, including severe acute respiratory syndrome coronavirus 2
77 (SARS-CoV-2),³⁵ African swine fever virus (ASFV),³⁶ human immunodeficiency
78 virus (HIV),³⁷ displaying obvious advantages of mild conditions, operational
79 simplicity, great sensitivity, and potent signal amplification.^{38, 39} Currently, the
80 CRISPR/Cas12a-based MPXV assay has not been systematically reported. According
81 to the best of our knowledge, there is only one short letter discussed the possibility
82 of implementing CRISPR technology in MPXV detection, while details on
83 pre-amplification, probe screening, analytical performance, and point-of-care testing
84 (POCT) have not been included.⁴⁰

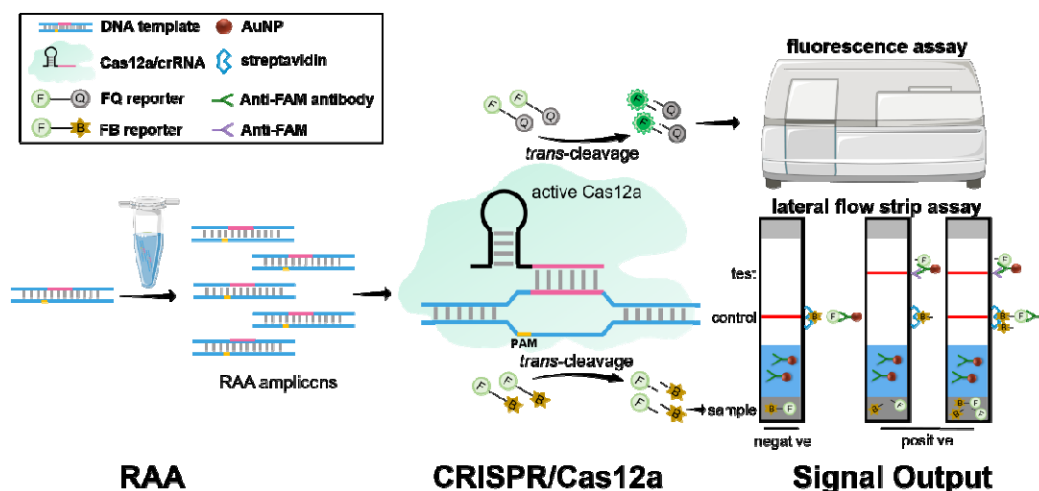
85 Herein, we proposed an ultrasensitive and rapid MPXV assay that integrates
86 recombinase-aided amplification (RAA) with CRISPR/Cas12a (the
87 RAA-Cas12a-MPXV assay) for the first time. After RAA pre-amplification of DNA
88 templates (containing MPXV *F3L* gene), CRISPR/Cas12a-based amplicon
89 recognition, and rapid cleavage of reporters, ultrasensitive detection of MPXV down
90 to 10¹ copies/μL via fluorescence readout was accomplished, which is 1000-fold more
91 sensitive than PCR. For MPXV POCT, we chose lateral flow strip technology as the
92 reliable interpretation of the assay and achieved the detection limit of 10⁴ copies/μL.
93 Our RAA-Cas12a-MPXV assay has the potential to detect MPXV with excellent
94 sensitivity, and selectivity with the aid of basic heaters, providing a rapid, convenient,
95 visual method for on-site screening in low-resource regions.

96

97 **Results and Discussion**

98 **Principle and verification of RAA-Cas12a-MPXV Assay**

99 The principle of our RAA-Cas12a-MPXV assay is illustrated in Scheme 1. It
100 consists of three steps: RAA amplification, CRISPR/Cas12a cleavage, and signal
101 output. In the first step, RAA selecting the DNA template, the conserved region of
102 MPXV-specific *F3L* gene,⁴¹⁻⁴³ as the target sequence, produces numerous amplicons
103 enhanced the sensitivity of the assay. In the second step, crRNA-specific recognition
104 and binding of amplicons activate the *trans*-cleavage activity of Cas12a, resulting in a
105 large number of ssDNA reporters cleaved. Depending on different reporters, the third
106 step presents two modes of signal output, fluorescence assay for FQ reporters
107 (modified with 6-FAM at the 5' end and BHQ1 at the 3' end) and lateral flow strip
108 assay for FB reporters (modified with 6-FAM at the 5' end and biotin at the 3' end),
109 improving the suitability and usability of our RAA-Cas12a-MPXV assay. The
110 departure of fluorophores of FQ reporters from quenchers enables fluorescence assay
111 using a fluorescence reader. In lateral flow strip assay, biotin of FB reporters is
112 captured by streptavidin at the first line on the strip (control), while the
113 FAM/anti-FAM antibody/AuNP complex migrates toward the second line (test) and
114 bind to anti-FAM. The result is visible within 5 min after sample addition at room
115 temperature, and the appearance of red color at the test band is considered positive.



116

117 **Scheme 1.** The principle of RAA-Cas12a-MPXV assay proposed in this research.

118 RAA for DNA template amplification; CRISPR/Cas12a system for reporter cleavage;

119 fluorescence assay and lateral flow strip assay for detection signal output.

120 To assess the feasibility of our RAA-Cas12a-MPXV assay, we compared

121 fluorescence results with or without DNA templates, and RAA product. As shown in

122 Figure 1A, the control group without DNA templates brought no significant

123 fluorescence change (NTC, blue line), indicating that no RAA amplicon was

124 generated for recognition by subsequent CRISPR/Cas12a in the absence of DNA

125 templates. The blank control without RAA product also showed no fluorescent signal,

126 demonstrating that CRISPR/Cas12a system does not cleave reporters without

127 amplicons (NRP, black line). Accordingly, we excluded the possibility of false

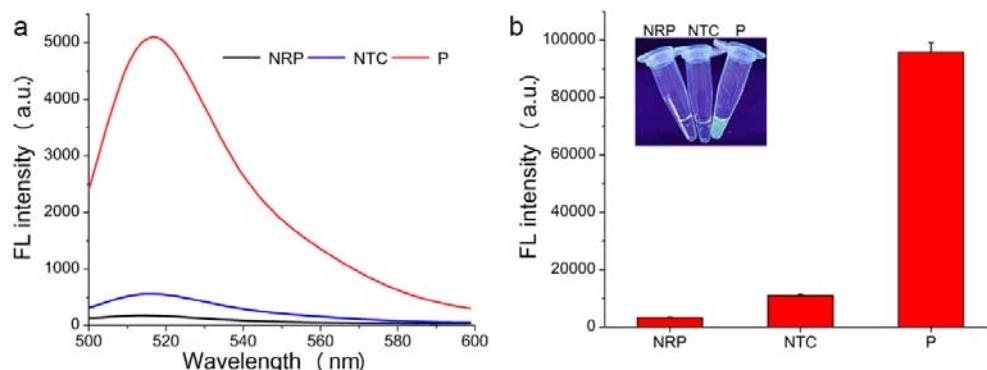
128 positive results due to contamination and non-specific amplification during RAA, as

129 well as non-specific cleavage of reporters during CRISPR/Cas12a. In contrast, in the

130 presence of DNA templates, RAA replicated numerous amplicons for crRNA

131 recognition and Cas12a activation, resulting in an intense fluorescence signal (red

132 line). The results obtained by the fluorescence reader were consistent with the
133 fluorescence spectroscopy (Figure 1B). Moreover, the fluorescence signal could be
134 observed by the naked eyes under ultraviolet (UV) light (Figure 1B, inset).

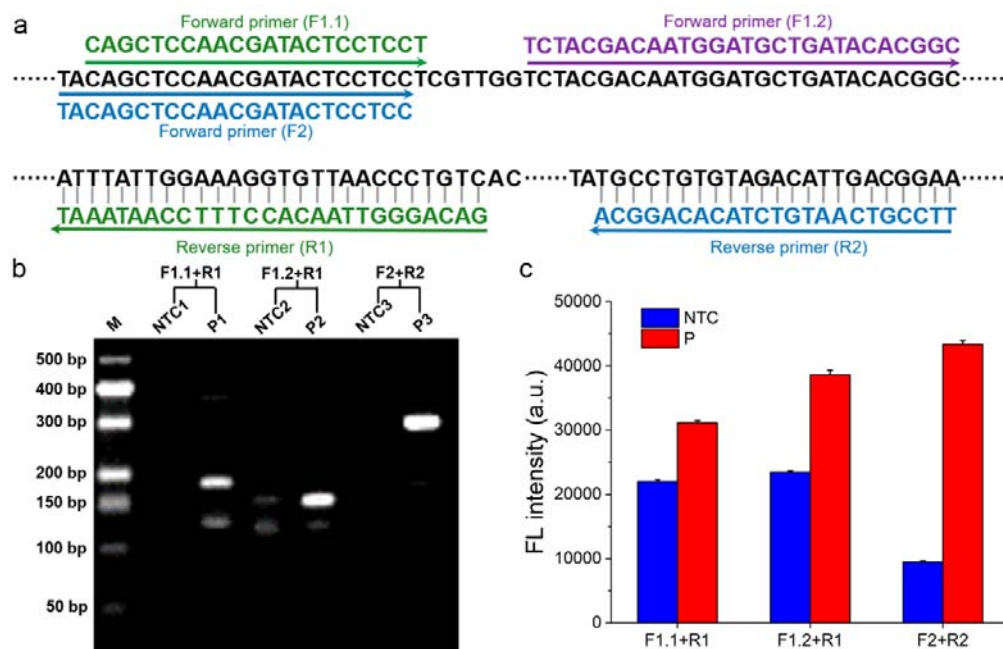


135
136 **Figure 1.** Verification of RAA-Cas12a-MPXV testing strategy. (a) Fluorescence
137 spectra of feasibility verification. (b) Fluorescence intensity of feasibility verification.
138 The inset was photographed by a smartphone under UV light. RAA was carried out
139 under 42 °C for 30 min using F2 and R2, then 1 μ L RAA product was added to 20 μ L
140 CRISPR/Cas12a reaction (50 nM Cas12a, 50 nM CrRNA, 1 μ M FQ reporter, 1 \times Cas
141 Buffer). NRP, no RAA product; NTC, no template control; P, positive.

142 Design and screening of RAA primers and Cas12a crRNA

143 RAA primers are the main factors affecting RAA amplification efficiency. To
144 obtain higher sensitivity and selectivity, three pairs of primers binding at different
145 sites of the MPXV-specific *F3L* gene were designed (Figure 2a, Table S1). Agarose
146 gel electrophoresis (AGE) and the RAA-Cas12a-MPXV fluorescence assay were
147 performed to screen the optimal primers for further experiments. The result of AGE
148 suggested that amongst the three pairs of RAA primers, only the third pair (F2+R2)

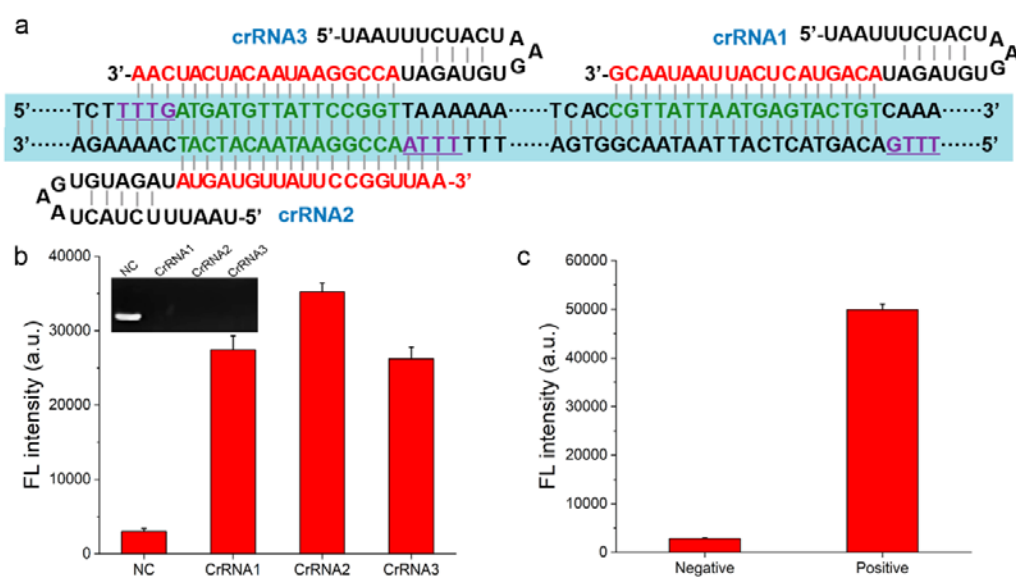
149 achieved the brightest specific amplification band while having no non-specific
 150 amplification band (Figure 2b). The fluorescence assay further confirmed F2 and R2
 151 as the most efficient primers, with the lowest fluorescence in NTC and the highest
 152 fluorescence in P (Figure 2c).



153
 154 **Figure 2.** Screening optimal primers for RAA. (a) The binding sites of designed
 155 primers on the DNA template. (b) AGE of RAA product. M, DNA marker; lane NTC1
 156 and P1, RAA products using F1.1 and R1; lane NTC2 and P2, RAA products using
 157 F1.2 and R1; lane NTC3 and P3, RAA products using F2 and R2. (c) Fluorescence
 158 intensity of RAA-CRISPR/Cas12a assay. NTC, no template control; P, positive.

159 Cas12a crRNA plays a central role in amplicon recognition and Cas12a
 160 activation, thus, to obtain the optimized crRNA that can potently activate Cas12a, we
 161 designed three crRNAs with the same length, while targeting to different sites on the
 162 RAA amplicon (Figure 3a). All of the crRNAs we designed activated Cas12a which

163 subsequently cis-cleaved amplicons (no bands in the insert of Figure 3b) and
 164 trans-cleaved FQ reporters (rising fluorescence in Figure 3b), while crRNA2 was the
 165 best candidate for its highest fluorescence intensity. With crRNA2-activating
 166 CRISPR/Cas12a, we observed a considerable fluorescence difference between the
 167 negative group and the positive group (Figure 3c). Consequently, we selected crRNA2
 168 for the following study.



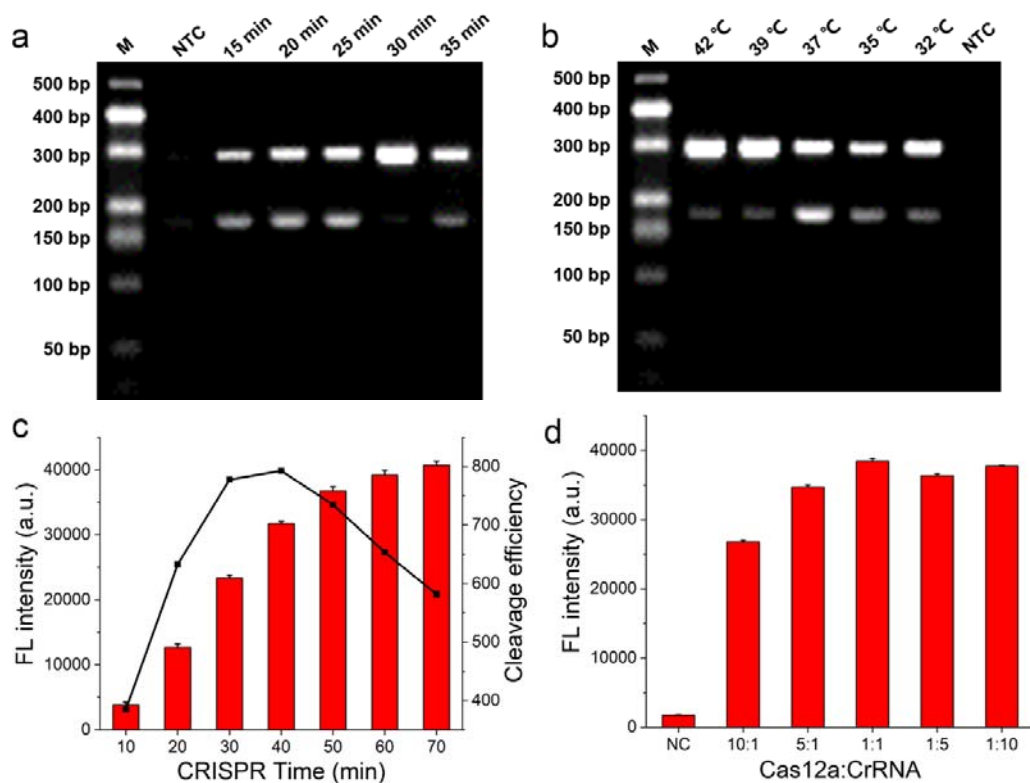
169
 170 **Figure 3.** Screening an optimal crRNA for CRISPR/Cas12a. (a) The binding sites of
 171 designed crRNAs on the DNA template (Green, crRNA binding sites; purple, PAM
 172 motifs). (b) Fluorescence intensity of CRISPR/Cas12a assay using different crRNAs.
 173 NC, no crRNA. The inset was an agarose gel image corresponding to different groups.
 174 Lane NC, CRISPR/Cas12a reaction products with no crRNA; lane crRNA1,
 175 CRISPR/Cas12a reaction products using crRNA1; lane crRNA2, CRISPR/Cas12a
 176 reaction products using crRNA2; lane crRNA3, CRISPR/Cas12a reaction products
 177 using crRNA3. (c) Fluorescence intensity of CRISPR/Cas12a assay using the

178 optimum crRNA2. Negative, without templates; positive, with templates.

179 **Optimization of the assay conditions**

180 To obtain optimal analytical performance of our RAA-Cas12a-MPXV assay,
181 several critical experimental conditions during RAA amplification and the
182 CRISPR/Cas12a system were optimized. We first optimized the temperature and
183 reaction time of RAA based on the optimal primers (F2 and R2). The band of 30-min
184 RAA was significantly brighter than that of other amplification times (Figure 4a), and
185 the fluorescence result reconfirmed 30 min as the ideal RAA reaction time (Figure S1).
186 Likewise, we chose 42 °C as the optimal temperature for RAA by combining the
187 results of electrophoresis and fluorescence assay (Figure 4b, Figure S1).

188 After the determination of RAA amplification conditions (42 °C, 30 min), we
189 further optimized the CRISPR/Cas12a system with crRNA2. We first investigated the
190 cleavage ability of Cas12a at different reaction times. The fluorescence intensity
191 spiked rapidly from the onset of the reaction to 40 min, and the cleavage efficiency
192 reached its maximum at 40 min, after which the fluorescence slowly increased (Figure
193 4c), thus, we chose 40 min as the best CRISPR reaction time. Furthermore, we
194 explored the effects of Cas12a:crRNA on the ultimate fluorescence intensity and
195 found that 1:1 was the optimal ratio (Figure 4d).



196

197 **Figure 4.** Optimization of the assay conditions. (a) The agarose gel image of RAA
198 amplification products under different reaction times (15 min, 20 min, 25 min, 30 min,
199 35 min). (b) The agarose gel image of RAA amplification products under different
200 temperatures (42 °C, 39 °C, 37 °C, 35 °C, 32 °C). NTC, no template control. (c)
201 Fluorescence intensity of CRISPR/Cas12a assay under different reaction times (10
202 min, 20 min, 30 min, 40 min, 50 min, 60 min, 70 min). Cleavage efficiency =
203 fluorescence intensity/CRISPR time. (d) Fluorescence intensity of CRISPR/Cas12a
204 assay using different ratios of Cas12a and crRNA (10:1, 5:1, 1:1, 1:5, 1:10). NC, no
205 crRNA.

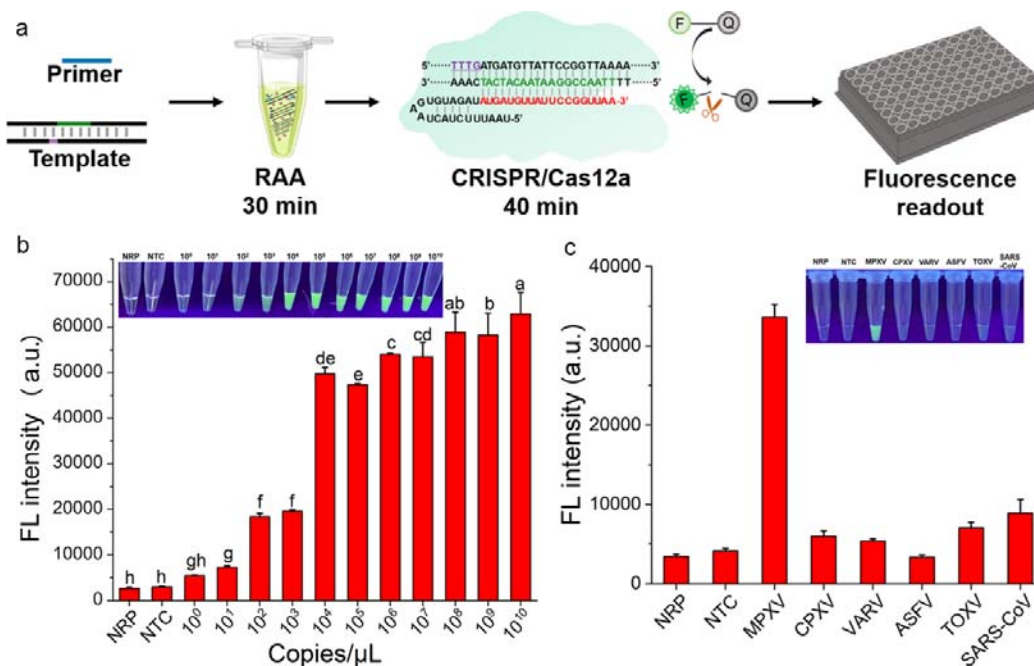
206 **Performances of the proposed RAA-Cas12a-MPXV fluorescence assay**

207 As shown in Figure 5a, our proposed RAA-Cas12a-MPXV fluorescence assay
208 has the merits of easy operation and rapid testing. To evaluate the sensitivity of the

209 fluorescence assay, DNA templates at serial dilution concentrations in the range of 10^0
210 to 10^{10} copies/ μL were subjected to RAA amplification, and then a 1 μL amplification
211 product was taken for the CRISPR/Cas12a reaction. The resulting fluorescence
212 intensity in Figure 5a exhibited that compared to the control group without the DNA
213 template and RAA product, the difference initiated in the group of 10^1 copies/ μL , and
214 gradually widened in the following groups, hence the limit of detection (LOD) of the
215 RAA-Cas12a-MPXV fluorescence assay was 10^1 copies/ μL . Additionally, we
216 achieved the LOD of 10^2 copies/ μL via naked-eye observation under UV light (Figure
217 5b, insert). We also evaluated the sensitivity of the PCR-Cas12a-MPXV fluorescence
218 assay (detailed in Supporting Information). In comparison with the
219 PCR-Cas12a-MPXV fluorescence assay, the LOD of which was 10^4 copies/ μL (Figure
220 S2), the RAA-Cas12a-MPXV fluorescence assay we established achieved 1000-fold
221 lower LOD, performing outstanding sensitivity. The higher sensitivity of RAA-based
222 assay is ascribed to the higher amplification efficiency of RAA and the better
223 compatibility of RAA to CRISPR.⁴⁴⁻⁴⁶

224 The selectivity of our RAA-Cas12a-MPXV fluorescence assay was next assessed
225 by comparing the fluorescence intensity produced by MPXV with that produced by
226 other viruses: cowpox virus (CPXV), variola virus (VARV), ASFV, and *Toxoplasma*
227 *Gondii* virus (TOXV), SARS-CoV-2. Both fluorescence values and naked-eye
228 observation demonstrated that only the MPXV group induced enhanced fluorescence
229 while other orthopox viruses (CPXV and VARV), and current high-profile viruses
230 (ASFV, TOXV, SARS-CoV-2) showed no fluorescence changes (Figure 5c). These

231 results confirmed the superior selectivity of our strategy toward MPXV, which is
 232 derived from the outstanding specificity of RAA amplification and Cas12a
 233 recognition.⁴⁷⁻⁴⁹



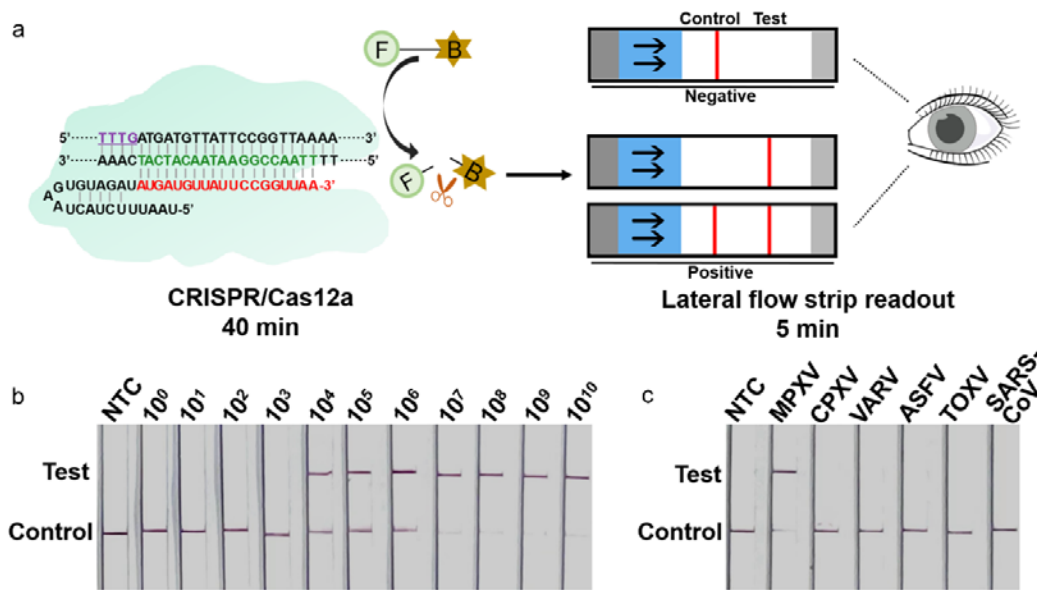
234
 235 **Figure 5.** Performances of the RAA-Cas12a-MPXV fluorescence assay. (a) Flowchart
 236 of the fluorescence assay. (b) Fluorescence intensity responding to a serial 10-fold
 237 dilution (10^{10-0} copies/ μL) of DNA templates in the sensitivity evaluation. The inset
 238 was photographed by a smartphone under UV light. Copy numbers and serial dilution
 239 values that are significantly different from each other are labeled with different
 240 lowercase letters above the error bars ($p < 0.05$). (c) Fluorescence intensity
 241 responding to MPXV, CPXV, VARV, ASFV, TOXV, and SARA-CoV-2 in the
 242 selectivity evaluation. The inset was photographed by a smartphone under UV light.
 243 NRP, no RAA product; NTC, no template control.

244 **RAA-Cas12a-MPXV Lateral Flow Strip Assay for Point-of-Care Testing**

245 To enable POCT, we designed the FB reporter as a substitute for the FQ reporter
246 of the fluorescence assay and established the RAA-Cas12a-MPXV lateral flow strip
247 assay (Figure 6a). Upon the addition of the reaction solution containing both intact FB
248 reporters and cracked FAMs and biotins at the sample pad, the anti-FAM
249 antibody/AuNP complexes quickly bound to the isolated FAMs as well as the intact
250 FB reporters as the sample migrated forward. Subsequently, the streptavidin, which
251 was immobilized at the control band, captured the cracked biotins and the FB
252 reporter/anti-FAM antibody/AuNP complexes, so that the control band appeared red
253 owing to the aggregation of AuNPs. The rest isolated FAM/anti-FAM antibody/AuNP
254 complexes migrated toward the test band and were captured by the FAM antibodies,
255 appearing red. Once there were enough amplicons to activate Cas12a to cleave all FB
256 reporters at maximum capacity, the color change would only appear at the test band as
257 a result. In brief, the color change appearing at the test band only or both the control
258 band and the test band indicated a positive result. In the negative group, the absence
259 of the DNA templates led to no amplicons for Cas12a activation and reporters
260 cleavage, consequently, the red color appeared only at the control band.

261 In the sensitivity assessment, with the increasing number of DNA templates,
262 amplicons for crRNA recognition and Cas12a activation incrementally grew via RAA,
263 eventually leading to a growing number of FB reporters being cleaved into FAM and
264 biotin, allowing the result that the color became darker at the test band and became
265 lighter at the control band presented on the lateral flow strips. Through naked-eye
266 observation, our RAA-Cas12a-MPXV lateral flow strip assay achieved the LOD of

267 10^4 copies/ μL (Figure 6b). Besides, this lateral flow strip assay showed great
268 selectivity, as demonstrated by the cross-reactivity test with other orthopox viruses
269 and current high-profile viruses (Figure 6c).



270

271 **Figure 6.** Performances of the RAA-Cas12a-MPXV lateral flow strip assay. (a)
272 Flowchart of the lateral flow strip assay. (b) Lateral flow strip results responding to a
273 serial 10-fold dilution (10^{10-0} copies/ μL) of DNA templates in the sensitivity
274 evaluation. (c) Lateral flow strip results responding to MPXV, CPXV, VARV, ASFV,
275 TOXV, and SARA-CoV-2 in the selectivity evaluation. NTC, no template control.

276

277 **Conclusions**

278 In this work, we established an RAA-Cas12a-MPXV assay for ultrasensitive,
279 facile, and rapid detection of MPXV by integrating RAA amplification with
280 CRISPR/Cas12a system and outputting the detection signal in the form of
281 fluorescence or lateral flow strip. Compared to current methods reported for detecting
282 MPXV, our RAA-Cas12a-MPXV assay possessed its notable strengths: (1) our assay
283 was carried out at a gentle temperature throughout, getting rid of the restraints of
284 thermal cycling processes and expensive instruments; (2) compared to the
285 conventional PCR with the LOD of 10^4 copies/ μL , our assay exhibited a significantly
286 improved detection limit of 10^1 copies/ μL in the fluorescence assay, 1000-fold more
287 sensitive than PCR. Meanwhile, visualized detection was realized with the LOD of
288 10^2 copies/ μL via UV light, and 10^4 copies/ μL via lateral flow strip; (3) combining the
289 lateral flow strip enabled us to perform on-site detection via naked eyes within 5 min
290 at room temperature with no need for any lab equipment, revealing the POCT
291 potential for screening MPXV in low-equipment scenario. Overall, the
292 RAA-Cas12a-MPXV assay is a promising method for MPXV detection with
293 outstanding sensitivity, selectivity, and portability.

294

295 **Experimental section**

296 **Materials and Reagents**

297 The oligonucleotides used in this study were synthesized and purified by Sangon
298 Biotech (Shanghai, China) and listed in Table S1. The monkeypox virus *F3L* plasmid
299 was purchased from Sangon Biotech. The RAA nucleic acid amplification kit
300 (S001ZC) was purchased from ZC Bioscience (Hangzhou, China). The 2 × Taq
301 Master Mix (P111) for PCR and the fastpure gel DNA extraction mini kit (DC301)
302 were provided from Vazyme Biotech (Nanjing, China). The Cas12a nuclease was
303 expressed and purified by our laboratory, details were provided in the supporting
304 information. Reagents in the 10 × Cas Buffer (500 mM NaCl, 100 mM Tris-HCl, 100
305 mM MgCl₂, 1 mg/mL BSA, pH 7.9) were purchased from Aladdin (Shanghai, China).
306 The lateral flow strip was purchased from IVD Biotech Service Center (Shanghai,
307 China).

308 **Primers and crRNAs Design**

309 The MPXV *F3L* gene sequence in this study was derived from German strain
310 MPXV-BY-IMB25241 (GenBank: ON568298) in May 2022 and American strain
311 MPXV-USA-2022-MA001 (GenBank: ON563414) during the same period, the
312 difference of which from Zaire strain Zaire-96-I-16 (NCBI Gene ID: 928998) was a
313 partial site mutation. Referring to the previously reported PCR primers for Zaire
314 strains with some changes,⁵⁰ we designed three pairs of RAA primers and screened
315 out the best primers in the follow-up. Cas12a crRNA consisted of a repeat sequence
316 and a amplicon -specific sequence. We designed three 19-nt crRNAs without the PAM

317 motif (TTTN), while the PAM motif appeared at the 5' end of the non-complementary
318 DNA sequence being targeted.

319 **Plasmid Construction and Amplification**

320 The gene sequences of CPXV, VARV, ASFV, and *Toxoplasma Gondii* virus
321 (TOXV) were retrieved from GenBank under accession number X75158, AY552594,
322 MN809121 and AF146527, then cloned into PUC57 vectors (Sangon, China) to create
323 the recombinant plasmids. After transformation into *E. coli* DH5 α and expansion
324 overnight, the recombinant plasmids were extracted using AxyPrep plasmid DNA
325 mini kit (AP-MN-P-50) purchased from Axygen Biotech (Hangzhou, China). The
326 concentrations of extracted plasmids were determined with NanoDrop 2000 (Thermo
327 Fisher, United States).

328 **Recombinase-Aided Amplification Reaction**

329 RAA reaction was performed with the RAA nucleic acid amplification kit,
330 following the manufacturer's instructions. Explicitly, the reaction powder was
331 dissolved with a mixture containing 5 μ L A Buffer (provided in the kit), 0.4 μ L each
332 of 10 μ M forward primer and reverse primer, and 2.7 μ L ddH₂O. Then, 1 μ L DNA
333 template and 0.5 μ L B Buffer (provided in the kit) were added into the reaction tube
334 and mixed gently, followed by incubation at 42 °C for 30 min. The DNA template was
335 replaced by ddH₂O in no template control (NTC) reaction. RAA products were
336 verified by 3 % AGE after purification by the fastpure gel DNA extraction mini kit.
337 The optimum primers for RAA were screened under the observation of the brightness
338 of the specific bands and the absence of non-specific bands after electrophoresis.

339 **RAA-Cas12a-MPXV Fluorescence Assay**

340 The RAA-Cas12a-MPXV fluorescence assay was performed in a 20 μ L system
341 containing 1 \times Cas Buffer, 50 nM crRNA, 50 nM Cas12a, 1 μ M FQ reporter, and 1 μ L
342 RAA product. Cas12a and crRNA were pre-conjugated in Cas Buffer at 37 $^{\circ}$ C for 10
343 min to facilitate cleavage performance of Cas12a. After the addition of FQ and RAA
344 product, the CRISPR reaction was incubated at 37 $^{\circ}$ C for 40 min and observed under
345 the FAM channel of the BioTek Synergy H1M microplate reader (Bio-Tek, United
346 States). In no RAA product (NRP) reaction, ddH₂O was in place of the RAA product.

347 **RAA-Cas12a-MPXV Lateral Flow Strip Assay**

348 The reaction system of the RAA-Cas12a-MPXV lateral flow strip assay was
349 similar to the fluorescence assay above, except for the replacement of the FQ with the
350 FB reporter. After incubation at 37 $^{\circ}$ C for 40 min, sterile ddH₂O was added to make
351 up the reaction system to 50 μ L for the insertion of the lateral flow strip. The result
352 was visualized after 5 min incubation at room temperature. The color appeared only at
353 the control band, indicating a negative result, and the color appeared at the test band
354 or both bands, indicating a positive result.

355 **Statistical Analysis**

356 Software OriginPro 2021 (OriginLab, Northampton, MA) was used for statistical
357 analyses and graphs. Data were shown as the average \pm standard deviation (n = 3).
358 Error bars represent the standard deviation from three independent experiments.

359

360 **Acknowledgments**

361 This work was supported by grants from the Natural Science Foundation of
362 Jiangsu Province (No. BK20200718 to B.Li), the Natural Science Foundation of the
363 Jiangsu Higher Education Institutions of China (20KJB350010 to B.Li), Jiangsu
364 Innovation and Entrepreneurship Doctoral Program to X.Zhang, and Jiangsu
365 Specially-Appointed Professor Project to X.Zhang.

366 **Conflict of Interest Disclosure**

367 The authors declare no competing financial interest.

368

369 **References**

- 370 (1) Xiang, Y.; White, A. Monkeypox virus emerges from the shadow of its more
371 infamous cousin: family biology matters. *Emerg Microbes Infec* **2022**, *11* (1),
372 1768-1777.
- 373 (2) Bunge, E. M.; Hoet, B.; Chen, L.; Lienert, F.; Weidenthaler, H.; Baer, L. R.;
374 Steffen, R. The changing epidemiology of human monkeypox-A potential threat? A
375 systematic review. *PLoS Negl Trop Dis* **2022**, *16* (2), e0010141.
- 376 (3) Organization, W. H. *Monkeypox*. 2022.
377 <https://www.who.int/news-room/fact-sheets/detail/monkeypox>.
- 378 (4) Lai, C. C.; Hsu, C. K.; Yen, M. Y.; Lee, P. I.; Ko, W. C.; Hsueh, P. R. Monkeypox:
379 An emerging global threat during the COVID-19 pandemic. *J Microbiol Immunol*
380 *Infect* **2022**. DOI: 10.1016/j.jmii.2022.07.004.
- 381 (5) McFadden, G. Poxvirus tropism. *Nat Rev Microbiol* **2005**, *3* (3), 201-213.
- 382 (6) Plowright, R. K.; Parrish, C. R.; McCallum, H.; Hudson, P. J.; Ko, A. I.; Graham,
383 A. L.; Lloyd-Smith, J. O. Pathways to zoonotic spillover. *Nat Rev Microbiol* **2017**, *15*
384 (8), 502-510.
- 385 (7) Murphy, H.; Ly, H. The potential risks posed by inter- and intraspecies
386 transmissions of monkeypox virus. *Virulence* **2022**, *13* (1), 1681-1683.
- 387 (8) Di Giulio, D. B.; Eckburg, P. B. Human monkeypox: an emerging zoonosis.
388 *Lancet Infect Dis* **2004**, *4* (1), 15-25.
- 389 (9) Reed, K. D.; Melski, J. W.; Graham, M. B.; Regnery, R. L.; Sotir, M. J.; Wegner,
390 M. V.; Kazmierczak, J. J.; Stratman, E. J.; Li, Y.; Fairley, J. A.; et al. The detection of

- 391 monkeypox in humans in the Western Hemisphere. *N Engl J Med* **2004**, *350* (4),
392 342-350.
- 393 (10) Rimoin, A. W.; Mulembakani, P. M.; Johnston, S. C.; Lloyd Smith, J. O.; Kisalu,
394 N. K.; Kinkela, T. L.; Blumberg, S.; Thomassen, H. A.; Pike, B. L.; Fair, J. N.; et al.
395 Major increase in human monkeypox incidence 30 years after smallpox vaccination
396 campaigns cease in the Democratic Republic of Congo. *Proc Natl Acad Sci U S A*
397 **2010**, *107* (37), 16262-16267.
- 398 (11) Durski, K. N.; McCollum, A. M.; Nakazawa, Y.; Petersen, B. W.; Reynolds, M.
399 G.; Briand, S.; Djingarey, M. H.; Olson, V.; Damon, I. K.; Khalakdina, A. Emergence
400 of Monkeypox - West and Central Africa, 1970-2017. *MMWR Morb Mortal Wkly Rep*
401 **2018**, *67* (10), 306-310.
- 402 (12) Erez, N.; Achdout, H.; Milrot, E.; Schwartz, Y.; Wiener-Well, Y.; Paran, N.; Politi,
403 B.; Tamir, H.; Israely, T.; Weiss, S.; et al. Diagnosis of Imported Monkeypox, Israel,
404 2018. *Emerg Infect Dis* **2019**, *25* (5), 980-983.
- 405 (13) Hobson, G.; Adamson, J.; Adler, H.; Firth, R.; Gould, S.; Houlihan, C.; Johnson,
406 C.; Porter, D.; Rampling, T.; Ratcliffe, L.; et al. Family cluster of three cases of
407 monkeypox imported from Nigeria to the United Kingdom, May 2021. *Euro Surveill*
408 **2021**, *26* (32), 2100745.
- 409 (14) Vaughan, A.; Aarons, E.; Astbury, J.; Balasegaram, S.; Beadsworth, M.; Beck, C.
410 R.; Chand, M.; O'Connor, C.; Dunning, J.; Ghebrehewet, S.; et al. Two cases of
411 monkeypox imported to the United Kingdom, September 2018. *Euro Surveill* **2018**,
412 *23* (38), 2-6.

- 413 (15) Ng, O. T.; Lee, V.; Marimuthu, K.; Vasoo, S.; Chan, G. H.; Lin, R. T. P.; Leo, Y. S.
414 A case of imported Monkeypox in Singapore. *Lancet Infect Dis* **2019**, *19* (11),
415 1166-1166.
- 416 (16) Rao, A. K.; Schulte, J.; Chen, T. H.; Hughes, C. M.; Davidson, W.; Neff, J. M.;
417 Markarian, M.; Delea, K. C.; Wada, S.; Liddell, A.; et al. Monkeypox in a Traveler
418 Returning from Nigeria - Dallas, Texas, July 2021. *Mmwr-Morbid Mortal W* **2022**, *71*
419 (14), 509-516.
- 420 (17) Costello, V.; Sowash, M.; Gaur, A.; Cardis, M.; Pasieka, H.; Wortmann, G.;
421 Ramdeen, S. Imported Monkeypox from International Traveler, Maryland, USA, 2021
422 (Response). *Emerg Infect Dis* **2022**, *28* (8), 1738-1738.
- 423 (18) Yinka-Ogunleye, A.; Aruna, O.; Dalhat, M.; Ogoina, D.; McCollum, A.; Disu, Y.;
424 Mamadu, I.; Akinpelu, A.; Ahmad, A.; Burga, J.; et al. Outbreak of human
425 monkeypox in Nigeria in 2017-18: a clinical and epidemiological report. *Lancet Infect*
426 *Dis* **2019**, *19* (8), 872-879.
- 427 (19) Organization, W. H. *2022 Monkeypox Outbreak: Global Trends*. 2022.
428 https://worldhealthorg.shinyapps.io/mpx_global/.
- 429 (20) Huhn, G. D.; Bauer, A. M.; Yorita, K.; Graham, M. B.; Sejvar, J.; Likos, A.;
430 Damon, I. K.; Reynolds, M. G.; Kuehnert, M. J. Clinical characteristics of human
431 monkeypox, and risk factors for severe disease. *Clin Infect Dis* **2005**, *41* (12),
432 1742-1751.
- 433 (21) Dzobo, M.; Gwinji, P. T.; Murewanhema, G.; Musuka, G.; Dzinamarira, T.
434 Stigma and public health responses: Lessons learnt from the COVID-19 pandemic to

- 435 inform the recent monkeypox outbreak. *Public Health Pract (Oxf)* **2022**, *4*, 100315.
- 436 (22) Li, Y.; Zhao, H.; Wilkins, K.; Hughes, C.; Damon, I. K. Real-time PCR assays for
437 the specific detection of monkeypox virus West African and Congo Basin strain DNA.
438 *J Virol Methods* **2010**, *169* (1), 223-227.
- 439 (23) Chelsky, Z. L.; Dittmann, D.; Blanke, T.; Chang, M.; Vormittag-Nocito, E.;
440 Jennings, L. J. Validation Study of a Direct Real-Time PCR Protocol for Detection of
441 Monkeypox Virus. *J Mol Diagn* **2022**. DOI: 10.1016/j.jmoldx.2022.09.001.
- 442 (24) Huggett, J. F.; French, D.; O'Sullivan, D. M.; Moran-Gilad, J.; Zumla, A.
443 Monkeypox: another test for PCR. *Euro Surveill* **2022**, *27* (32).
- 444 (25) Karem, K. L.; Reynolds, M.; Braden, Z.; Lou, G.; Bernard, N.; Patton, J.; Damon,
445 I. K. characterization of acute-phase humoral immunity to monkeypox: use of
446 immunoglobulin M enzyme-linked immunosorbent assay for detection of monkeypox
447 infection during the 2003 North American outbreak. *Clin Diagn Lab Immunol* **2005**,
448 *12* (7), 867-872.
- 449 (26) Dubois, M. E.; Hammarlund, E.; Slifka, M. K. Optimization of peptide-based
450 ELISA for serological diagnostics: a retrospective study of human monkeypox
451 infection. *Vector Borne Zoonotic Dis* **2012**, *12* (5), 400-409.
- 452 (27) Iizuka, I.; Saijo, M.; Shiota, T.; Ami, Y.; Suzuki, Y.; Nagata, N.; Hasegawa, H.;
453 Sakai, K.; Fukushi, S.; Mizutani, T.; et al. Loop-mediated isothermal
454 amplification-based diagnostic assay for monkeypox virus infections. *J Med Virol*
455 **2009**, *81* (6), 1102-1108.
- 456 (28) Ryabinin, V. A.; Shundrin, L. A.; Kostina, E. B.; Laassri, M.; Chizhikov, V.;

- 457 Shchelkunov, S. N.; Chumakov, K.; Sinyakov, A. N. Microarray assay for detection
458 and discrimination of Orthopoxvirus species. *J Med Virol* **2006**, *78* (10), 1325-1340.
- 459 (29) Kostina, E. V.; Sinyakov, A. N.; Ryabinin, V. A. A many probes-one spot
460 hybridization oligonucleotide microarray. *Anal Bioanal Chem* **2018**, *410* (23),
461 5817-5823.
- 462 (30) Altindis, M.; Puca, E.; Shapo, L. Diagnosis of monkeypox virus - An overview.
463 *Travel Med Infect Dis* **2022**, *50*, 102459.
- 464 (31) Edghill-Smith, Y.; Golding, H.; Manischewitz, J.; King, L. R.; Scott, D.; Bray, M.;
465 Nalca, A.; Hooper, J. W.; Whitehouse, C. A.; Schmitz, J. E.; et al. Smallpox
466 vaccine-induced antibodies are necessary and sufficient for protection against
467 monkeypox virus. *Nat Med* **2005**, *11* (7), 740-747.
- 468 (32) Berthet, N.; Dickinson, P.; Filliol, I.; Reinhardt, A. K.; Batejat, C.; Vallaey, T.;
469 Kong, K. A.; Davies, C.; Lee, W.; Zhang, S.; et al. Massively parallel pathogen
470 identification using high-density microarrays. *Microb Biotechnol* **2008**, *1* (1), 79-86.
- 471 (33) Li, S. Y.; Cheng, Q. X.; Wang, J. M.; Li, X. Y.; Zhang, Z. L.; Gao, S.; Cao, R. B.;
472 Zhao, G. P.; Wang, J. CRISPR-Cas12a-assisted nucleic acid detection. *Cell Discov*
473 **2019**, *5* (1), 1.
- 474 (34) Xiong, Y.; Zhang, J.; Yang, Z.; Mou, Q.; Ma, Y.; Xiong, Y.; Lu, Y. Functional
475 DNA Regulated CRISPR-Cas12a Sensors for Point-of-Care Diagnostics of
476 Non-Nucleic-Acid Targets. *J Am Chem Soc* **2020**, *142* (1), 207-213.
- 477 (35) Xie, S.; Qin, C.; Zhao, F.; Shang, Z.; Wang, P.; Sohail, M.; Zhang, X.; Li, B. A
478 DNA-Cu nanocluster and exonuclease I integrated label-free reporting system for

- 479 CRISPR/Cas12a-based SARS-CoV-2 detection with minimized background signals. *J*
480 *Mater Chem B* **2022**, *10* (32), 6107-6117.
- 481 (36) Xie, S.; Tao, D.; Fu, Y.; Xu, B.; Tang, Y.; Steinaa, L.; Hemmink, J. D.; Pan, W.;
482 Huang, X.; Nie, X.; et al. Rapid Visual CRISPR Assay: A Naked-Eye Colorimetric
483 Detection Method for Nucleic Acids Based on CRISPR/Cas12a and a Convolutional
484 Neural Network. *Acs Synth Biol* **2022**, *11* (1), 383-396.
- 485 (37) Pang, Y.; Li, Q.; Wang, C.; Zhen, S.; Sun, Z.; Xiao, R. CRISPR-cas12a mediated
486 SERS lateral flow assay for amplification-free detection of double-stranded DNA and
487 single-base mutation. *Chem Eng J* **2022**, *429*, 132109.
- 488 (38) Chen, J. S.; Ma, E.; Harrington, L. B.; Da Costa, M.; Tian, X.; Palefsky, J. M.;
489 Doudna, J. A. CRISPR-Cas12a target binding unleashes indiscriminate
490 single-stranded DNase activity. *Science* **2018**, *360* (6387), 436-439.
- 491 (39) Liang, M.; Li, Z.; Wang, W.; Liu, J.; Liu, L.; Zhu, G.; Karthik, L.; Wang, M.;
492 Wang, K. F.; Wang, Z.; et al. A CRISPR-Cas12a-derived biosensing platform for the
493 highly sensitive detection of diverse small molecules. *Nat Commun* **2019**, *10* (1),
494 3672.
- 495 (40) Sui, Y.; Xu, Q.; Liu, M.; Zuo, K.; Liu, X.; Liu, J. CRISPR-Cas12a-based
496 detection of monkeypox virus. *J Infect* **2022**. DOI: 10.1016/j.jinf.2022.08.043.
- 497 (41) Kim, J. W.; Lee, M.; Shin, H.; Choi, C. H.; Choi, M. M.; Kim, J. W.; Yi, H.; Yoo,
498 C. K.; Rhie, G. E. Isolation and identification of monkeypox virus
499 MPXV-ROK-P1-2022 from the first case in the Republic of Korea. *Osong Public*
500 *Health Res Perspect* **2022**, *13* (4), 308-311.

- 501 (42) Gong, Q.; Wang, C.; Chuai, X.; Chiu, S. Monkeypox virus: a re-emergent threat
502 to humans. *Virologica Sinica* **2022**, *37* (4), 477-482.
- 503 (43) Feng, J.; Xue, G.; Cui, X.; Du, B.; Feng, Y.; Cui, J.; Zhao, H.; Gan, L.; Fan, Z.;
504 Fu, T.; et al. Development of a Loop-Mediated Isothermal Amplification Method for
505 Rapid and Visual Detection of Monkeypox Virus. *Microbiol Spectr* **2022**, e0271422.
- 506 (44) Zhang, Y.; Li, Q.; Guo, J.; Li, D.; Wang, L.; Wang, X.; Xing, G.; Deng, R.; Zhang,
507 G. An Isothermal Molecular Point of Care Testing for African Swine Fever Virus
508 Using Recombinase-Aided Amplification and Lateral Flow Assay Without the Need
509 to Extract Nucleic Acids in Blood. *Front Cell Infect Microbiol* **2021**, *11*, 633763.
- 510 (45) Ma, Q. N.; Wang, M.; Zheng, L. B.; Lin, Z. Q.; Ehsan, M.; Xiao, X. X.; Zhu, X.
511 Q. RAA-Cas12a-Tg: A Nucleic Acid Detection System for *Toxoplasma gondii* Based
512 on CRISPR-Cas12a Combined with Recombinase-Aided Amplification (RAA).
513 *Microorganisms* **2021**, *9* (8), 1644.
- 514 (46) Zhang, A.; Sun, B.; Zhang, J.; Cheng, C.; Zhou, J.; Niu, F.; Luo, Z.; Yu, L.; Yu,
515 C.; Dai, Y.; et al. CRISPR/Cas12a Coupled With Recombinase Polymerase
516 Amplification for Sensitive and Specific Detection of *Aphelenchoides besseyi*. *Front*
517 *Bioeng Biotechnol* **2022**, *10*, 912959.
- 518 (47) Li, F.; Ye, Q.; Chen, M.; Zhou, B.; Zhang, J.; Pang, R.; Xue, L.; Wang, J.; Zeng,
519 H.; Wu, S.; et al. An ultrasensitive CRISPR/Cas12a based electrochemical biosensor
520 for *Listeria monocytogenes* detection. *Biosens Bioelectron* **2021**, *179*, 113073.
- 521 (48) Li, F.; Ye, Q.; Chen, M.; Xiang, X.; Zhang, J.; Pang, R.; Xue, L.; Wang, J.; Gu,
522 Q.; Lei, T.; et al. Cas12aFDet: A CRISPR/Cas12a-based fluorescence platform for

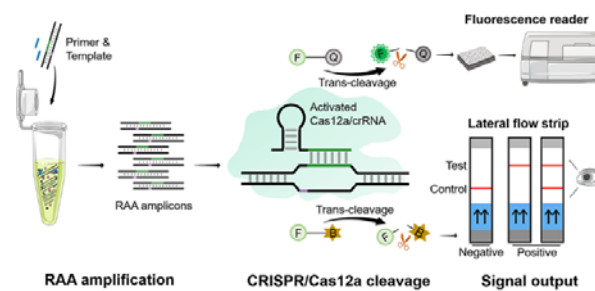
523 sensitive and specific detection of *Listeria monocytogenes* serotype 4c. *Anal Chim*
524 *Acta* **2021**, *1151*, 338248.

525 (49) Zhi, S.; Shen, J.; Li, X.; Jiang, Y.; Xue, J.; Fang, T.; Xu, J.; Wang, X.; Cao, Y.;
526 Yang, D.; et al. Development of Recombinase-Aided Amplification (RAA)-Exo-Probe
527 and RAA-CRISPR/Cas12a Assays for Rapid Detection of *Campylobacter jejuni* in
528 Food Samples. *J Agric Food Chem* **2022**, *70* (30), 9557-9566.

529 (50) Kulesh, D. A.; Loveless, B. M.; Norwood, D.; Garrison, J.; Whitehouse, C. A.;
530 Hartmann, C.; Mucker, E.; Miller, D.; Wasieloski, L. P., Jr.; Huggins, J.; et al.
531 Monkeypox virus detection in rodents using real-time 3'-minor groove binder TaqMan
532 assays on the Roche LightCycler. *Lab Invest* **2004**, *84* (9), 1200-1208.

533

534 **For TOC only**



535

536